

Slotted coaxial cavity resonator for head imaging at ultra high fields

Anna Andreychenko¹, Alexander J.E. Raaijmakers¹, Peter R. Luijten¹, Jan J.W. Lagendijk¹, and Cornelis A.T. van den Berg¹
¹Imaging Division, UMC Utrecht, Utrecht, Netherlands

Introduction: Waveguide slot antennas are popular directional antennas used in microwave engineering at UHF (>300 MHz) [1]. These antennas are robust and easy to design. The operational RF frequency of ultra high field MRI falls into this frequency range. Therefore such antenna types can be an alternative to the existing coil designs at ultra high field MRI. Here we propose a slotted coaxial cavity resonator designed for head imaging at 11.7 T and compare it to the conventional birdcage head coil.

Methods: The resonance frequency of the coaxial resonator is defined by its dimensions[2,3]: $f_{res} = \frac{c}{2\pi\sqrt{\mu_r\epsilon_r}} \sqrt{\left(\frac{1}{a+b}\right)^2 + \left(\frac{l\pi}{d}\right)^2}$, where a , b - inner, outer diameters, d -length of the resonator and l - number of half-

wavelengths. The dimensions of the coaxial cavity resonator were optimized to match the size requirements of the head coil diameter and at the same time to resonate at approximately 500 MHz. The resonator was created with two coaxial cylindrical metal sheets ($a=0.26\text{m}$, $b=0.32\text{m}$, $d=0.8\text{m}$). The space between the sheets was filled with air ($\epsilon_r=1$). One of the ends of the resonator was closed with a metal wall and the opposite end was left open (Fig. 1). The length of the resonator was chosen to include two half-wavelengths ($l=2$). Eight longitudinal equally spaced half-wavelength slots ($0.025\times0.4\text{m}$) were created in the inner conductor of the cavity (close to the open end) in order to radiate into the core of the resonator where the load was located. Eight ports (source impedance 50 Ohm), equally spaced along circumference, were placed between the outer and inner conductors of the coaxial resonator at a distance of 0.2 m from the closed end. The model of the slotted coaxial cavity resonator was created for FDTD simulations (SEMCAD, SPEAG, Zurich, Switzerland). First, broad band simulations (center frequency 500 MHz, bandwidth 200 MHz) were performed for the empty slotted coaxial cavity resonator. Then the resonator was loaded with a human model [4] (Fig. 2) and also the bore of the scanner (diameter 0.58 m) was included in the SEMCAD model for harmonic simulations. For comparison, a two-ports birdcage head coil (tuned to 11.7T and loaded with the same human model) was simulated.

Results: The S11 curve obtained from broad band simulations of one single port (Fig. 3) showed -12 dB damping at 504 MHz. This frequency was used for the following harmonic simulations. B_1^+ distributions (normalized to 1 W) of the individual ports (all source impedances were 50 Ohm) were simulated for the human head (Fig. 4, inset). The quadrature excitation of the ports showed a typical quadrature distribution in the head with a standing wave pattern that was, not surprisingly, more pronounced than at lower fields (Fig. 4&5B). The quadrature excitation of the birdcage model showed a very similar B_1^+ pattern in the head (Fig.5A). Based on the FDTD simulations of all the ports with quadrature phase settings, B_1^+ efficiency was evaluated. The maximum achievable B_1^+ for 1 W delivered power appeared to be 13 % higher than the birdcage coil: 0.54 uT/1W for the here proposed resonator and 0.48 uT/1W for the birdcage. RF safety was evaluated for the quadrature excitation of the slotted coaxial cavity resonator (Fig. 6 A): $B_1^{+2}/\text{SAR}_{10g} = 0.49 \text{ uT}^2/\text{W/kg}$, average SAR = 0.016 W/kg per 1 W delivered power and compared to the birdcage coil design: $B_1^{+2}/\text{SAR}_{10g} = 0.45 \text{ uT}^2/\text{W/kg}$, average SAR = 0.015 W/kg. The open end of the resonator did not create significant SAR deposition at the shoulders as could be expected and peak SAR values occurred in the head center. The power flow showed that the slots effectively directed the wave towards the head top and sides, while very little power leaked out from the open end (Fig. 6B). The presence of eight independent ports could be exploited for RF shimming of the entire transversal slice (Fig.7A) and even more efficiently for partial RF shimming (Fig.7 B).

Discussion & further developments: B_1^+ efficiency of the quadrature settings also included strong coupling between the ports (-8 dB to the closest port, -15 dB to the next neighbor and -20 dB to the third port, impedances of all sources were 50 Ohm). Remarkably, the longitudinal wavelength is defined by the dimensions of the resonator and can exceed the wavelength in free space. This can be exploited for a better longitudinal coverage. The shape of the slot can be arbitrary if its circumference fulfills the wavelength condition. Therefore, the shape of the slots can be adapted to tailor the B_1^+ distribution in head. Additionally, a dielectric ring can be placed next to the open end to modify the boundary conditions which can also influence the B_1^+ distribution. The spacing between the inner and outer cylinder can be filled with a higher permittivity material to adjust the resonating wavelength and dimensions. However, it should consist of a very low loss material to avoid additional losses. The strong wave effects in the head at 11.7T limit RF shimming possibilities for the entire slice. Nevertheless, TIAMO combination of two partially shimmed slices can be applied instead [5] providing a good homogeneity over the entire slice. This new antenna design could be feasible to apply at lower frequencies such as 7 and 9.4 T but the resonator would become larger, possibly unwieldy.

Conclusions: A cheap and easily manufactured design of the head coil at 11.7 T has been developed with good B_1^+ efficiency and RF shimming performance. This design can be an effective alternative to the existing coil designs.

References: [1] Jasik H, Antenna Engineering Handbook; [2] Pozar D, Microwave engineering, 1998; [3] Zhang K et al, Electromagnetic theory for microwaves and optoelectronics, 1998; [4] Christ A et al. Phys Med Biol 2010; [5] Orzada S et al, MRM 2010.

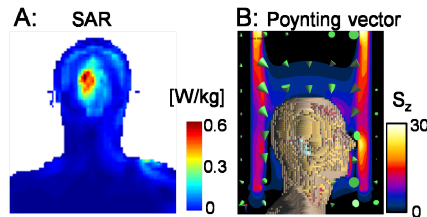


Figure 6. A: Coronal SAR distribution. Peak value occurs in the head center. B: Poynting vector. Z-component is shown with color scale. Power flow is mainly directed to the head (arrows).

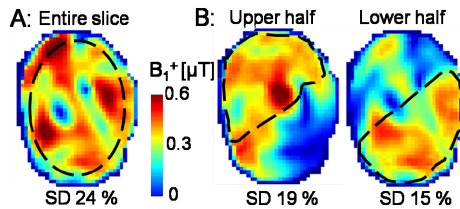


Figure 7. RF shimming performance of the eight ports for the entire transversal slice (A) and upper/lower halves (B). The shimmed regions are outlined with the dashed line and standard deviations are written below.

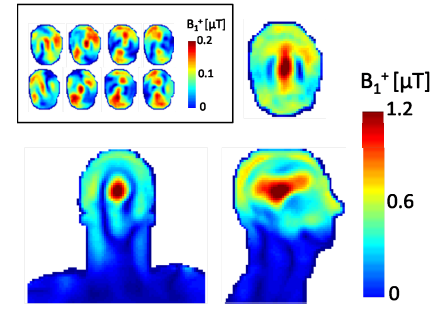


Figure 4. B_1^+ distributions in the head for quadrature combination of the eight ports. Inset: transversal B_1^+ distributions of individual ports normalized for 1 W delivered power.

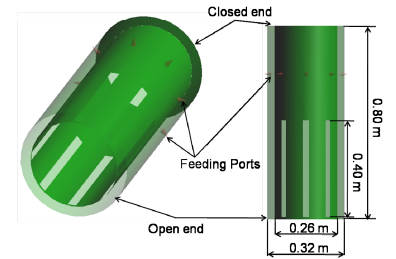


Figure 1. The slotted coaxial cavity resonator. Eight longitudinal slots were cut in the inner conductor.

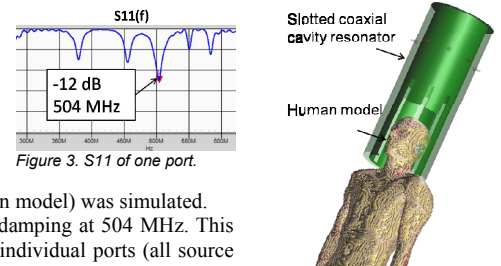


Figure 2. The slotted coaxial cavity resonator placed around head of human model.

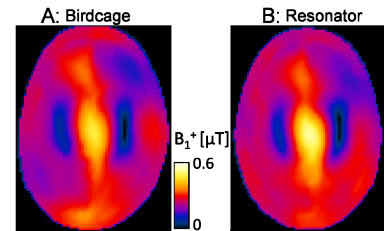


Figure 5. Normalized to 1 W transverse B_1^+ pattern in head for the birdcage coil (A) and for the slotted coaxial cavity resonator (B). Note a remarkable similarity of the patterns.